MATERIALS FORUM VOLUME 29 - Published 2005
Edited by J.F. Nie and M. Barnett



# POISONING AND FADING MECHANISM OF GRAIN REFINEMENT IN Al-7Si ALLOY

**S.A. Kori[1*], V. Auradi[1], B.S. Murty[2], M. Chakraborty[3]**
[1] R & D Centre, Dept. of Mech. Engg., B. E. C., Bagalkot - 587 102, Karnataka, India
[2] Dept. of Met. & Mater. Engg., Indian Institute of Technology Madras, Chennai - 600 036, India
[3] Dept. of Met. & Mater. Engg., Indian Institute of Technology, Kharagpur - 721 302, India

## ABSTRACT

The poisoning and fading mechanism of grain refinement in Al-7Si alloy has been studied in detail with the conventional (0.01%Ti or B) and higher addition levels of indigenously developed Al-3Ti, Al-5Ti, Al-3B and Al-5Ti-1B master alloys. Results suggest that on prolonged holding the melt after the conventional addition of grain refiner to Al-7Si alloy, size of the α-Al dendrites increases (fading), which could be due to the dissolution/settling of $TiAl_3$ and $AlB_2$ particles. However, vigorous agitation of the melt after prolonged holding (120s min.), can partly bring back the particles into the liquid melt and acts as heterogeneous nucleating sites to some limited extents (120s min. sample). In addition, the conventional addition (0.2 wt%) of Ti-rich Al-3Ti, Al-5Ti and Al-5Ti-1B master alloy to Al-7Si alloy, the Si from the melt reacts with grain refining constituents ($TiAl_3$) and formation of titanium silicide and coats on the surface of the $TiAl_3$ particles and poisons the effectiveness of the nuclei. However, the higher addition level of these master alloy or B-rich Al-3B master alloys can overcome poisoning effect of Al-7Si alloy.

## 1. INTRODUCTION

Hypoeutectic Al-Si alloys exhibiting good castability, high strength to weight ratio, better corrosion resistance, good weldability and better machinability and have been widely applied in aerospace, automotive, defence and marine sectors where they are used for cylinder blocks, piston heads and other engine body castings etc [1]. Hypoeutectic Al-Si alloys have a large fraction of primary α-Al in their microstructure. The mechanical properties of the hypoeutectic Al-Si alloys are strongly dependent on the size, the morphology and the distribution of eutectic silicon and the primary α-Al present in the microstructures. The improvement in the quality of the castings and their properties can be achieved by grain refinement which reduces the size of the primary α-Al grains in the casting, which otherwise solidifies with coarse columnar grain structure. A fine equiaxed structure leads to several benefits such as improved mechanical properties, improved feeding during solidification, reduced and more evenly distributed porosity, better dispersion of second phase, excellent deep drawability of the products, improved surface finish and other desired properties [2-3]. To achieve additional improvements in mechanical properties, modification is essential which converts large brittle flakes of silicon into fine fibres.

Grain refinement of hypoeutectic Al-Si alloys containing ≥7% Si is not a common industrial practice. These alloys are modified by Na or Sr to obtain fine eutectic Si in the microstructure. In order to accrue the advantages of grain refinement, some attempts have been made in the past to refine the α-Al dendrites in these alloys. However, during the grain refinement of these alloys, if the melt were held for a longer time after the addition of grain refiner, the casting would develop coarse grain structure, instead of otherwise fine grain structure, which is commonly known as *fading phenomenon*. Fading phenomenon may be attributed to either dissolution or settling/floating (or both) of nucleating particles during long holding [2]. In addition, some of these alloys contain Cr, Zr, Li and Si as alloying elements, which make them respond poorly to grain refinement by Al-Ti-B master alloy, is usually termed as *poisoning effect*. It is in general believed that the poisoning elements interact with the grain refining constituents of the Al-Ti-B master alloys ($TiAl_3$ and $TiB_2$) and make them ineffective or less effective [4-9].

During grain refinement of Al-Si alloys, when the addition levels of Si to Al is low, Si behaves as expected in reducing the grain size by what is termed constitutional or growth restriction effects. However, above approximately 3wt% Si the opposite is true and coarsening occurs. It has been suggested that the $TiB_2$ interface is an energetically favorable site for Si atoms, compared to the matrix subgrain/grain boundaries. Another factor, which could be of importance, is that the solubility of Ti in solid Al decreases with the presence of Si. The surface chemistry and hence surface energy are thought to adversely affect $TiB_2$ as nucleant [10]. Sigworth and Guzowaski [3] suggested that in case of grain refinement of Al-Si alloys titanium silicide coats on the surface of $TiAl_3$ and poison the effectiveness of the nuclei present in the Al-Ti master alloy. On the other hand, when Al-B is the grain refiner, they proposed that $AlB_2$ phase acts as the nucleant and the presence of Si improves its nucleation potential. Further, the enhanced performance of Al-3Ti-3B and Al-1Ti-3B master alloys when compared to Al-B master alloys was due to heterogeneous

nucleation on the $(Al,Ti)B_2$ phase, which is isomorphous with $AlB_2$. As $AlB_2$ and $(Al,Ti)B_2$ are isomorphous to $TiB_2$ all of them are expected to behave in a similar manner towards nucleation of Al. However, in reality B-rich Al-3B, Al-1Ti-3B and Al-3Ti-3B master alloys containing $AlB_2$ and $(Al,Ti)B_2$ particles perform more effectively for Al-7Si alloys than conventional Al-5Ti-1B master alloys containing $TiB_2$ and $TiAl_3$ particles [11-14]. Recently, an alternative mechanism has been proposed by Mohanty and Gruzeleski [15] for the grain refinement of Al-Si alloys. They proposed that the nucleation of Al in hypoeutectic Al-Si alloys occurs on the pre-existing α-Al, which forms by the eutectic reaction from the B-containing Al-melt. In the present study, an attempt has been made to investigate the poisoning and fading phenomenon involved in the grain refinement of Al-7Si alloy with conventional and higher addition levels of indigenously developed Al-3Ti, Al-5Ti, Al-3B and Al-5Ti-1B master alloys.

## 2. EXPERIMENTAL PROCEDURES

Binary Al-3Ti, Al-5Ti, Al-3B and ternary Al-5Ti-1B master alloys were prepared by the reaction of molten Aluminium with complex halide salts like $K_2TiF_6$ and or $KBF_4$ in an induction furnace at a reaction temperature of $800^0$C and with a reaction time of 60 min. The furnace temperature was controlled to an accuracy of $\pm5^0$C by a digital temperature controller. After the completion of the reaction (after 60 min.), the spent salt was decanted from the surface of the molten alloy and the alloy was cast. The master alloys so prepared were characterized by chemical analysis, XRD, scanning electron microscopy (SEM) and Energy dispersive x-ray (EDX) microanalysis. Table 1 shows the chemical compositions of the various master alloys, assessed using atomic absorption spectrophotometer (model AA-670, Shimadzu Japan).

*Table 1: Shows chemical composition of the various master alloys and cast alloys used in the present study*

| Nominal Composition | Composition (wt%) | | | | |
|---|---|---|---|---|---|
| | Ti | B | Si | Fe | Al |
| Al-3Ti | 3.00 | - | 0.26 | 0.20 | Bal |
| Al-3B | - | 2.7 | 0.086 | 0.15 | Bal |
| Al-5Ti | 5.01 | -- | 0.15 | 0.20 | Bal |
| Al-5Ti-1B | 5.01 | 1.00 | 0.15 | 0.20 | Bal |
| Al-7Si | -- | -- | 7.0 | 0.16 | Bal |

| Nominal Composition | Master alloy used | Addition levels (wt%) | Ti% | %B |
|---|---|---|---|---|
| Al-7Si | Al-3Ti | 0.35, 0.40, 0.45, 0.50, 0.55, 0.60, 0.65, 0.70 | 0.01, 0.012 0.013, 0.015, 0.016, 0.018, 0.019, 0.021 | -- |
| Al-7Si | Al-5Ti | 0.20, 0.275, 0.30, 0.325. 0.35, 0.40 | 0.012, 0.014 0.015, 0.016 0.017, 0.02 | -- |
| Al-7Si | Al-3B | 0.35, 0.40, 0.45, 0.50, 0.60, 0.65 | -- | 0.009, 0.011, 0.012, 0.013, 0.015, 0.016, 0.017 |
| Al-7Si | Al-5Ti-1B | 0.12*, 0.16, 0.20, 0.20, 0.24, 0.28, 0.32, 0.36, 0.40, 0.44, 0.48, 0.52 | 0 006*, 0.008, 0.01, 0.012, 0.014, 0.016, 0.018, 0.02, 0.022, 0.024, 0.028 | 0.0012*, 0.0016, 0.0020, 0.0024, 0.0028, 0.0032, 0.0036, 0.0040, 0.0044, 0.0048, 0.0052 |

***Addition level 0.12wt% = 0.006%Ti, 0.0012%B respectively***

*Table 2: Grain Refinement of Al-7Si alloy at 720℃ using conventional and higher addition levels of various binary and ternary master alloys*

Grain refinement studies of Al-7Si alloy have been carried out in a resistance furnace under a cover flux (45%NaCl+45%KCl+10%NaF) and the melt was held at 720°C. After degassing with solid hexachloroethane ($C_2Cl_6$), indigenously developed master alloy chips were added to the melt for grain refinement. The melt was stirred for 30 seconds with zircon coated iron rod after the addition of grain refiner, after which no further stirring was carried out. Parts of the melts were poured at regular intervals (0, 2, 5, 30, 60, 120 and 120s min.) into a cylindrical graphite mould (25mm dia and 100mm height) surrounded by fireclay brick with its top open for pouring. The samples designated as 0 min. refers to that part of the alloy melt which was cast before the addition of grain refiner and 120s min. refers to the sample with grain refiner, which was stirred after 120 min. casting for a period of 10 sec. Table 2 shows the details of grain refinement studies of Al-7Si alloy with different addition levels of various Al-3Ti, Al-5Ti, Al-3B and Al-5Ti-1B master alloys. The grain-refined samples were characterized by macroscopy using Poulton's reagent and microscopy by Keller's reagent. Selected samples were taken for DAS measurement using image analyser and characterized by using SEM/EDX microanalysis.

## 3. RESULTS AND DISCUSSION

### 3.1 SEM/EDX Microanalysis of Master Alloys

Figure 1a shows the SEM microphotograph of Al-3B master alloy synthesized at $800^0$C-60min. The figure clearly shows that the microstructure of Al-3B master alloy consists of hexagonal aluminium boride particles in an aluminium matrix. It may be noted that, the reaction temperature is below liquidus line of the Al-B phase diagram, at which molten Al and intermetallic particles are in equilibrium. The reaction proceeds at the $KBF_4$ salt-liquid Al interface. The release of B from $KBF_4$ salt should result in an instantaneous reaction with Al to form boride particles, as the solubility of B in liquid Al at the reaction temperature is negligible [12]. The $KBF_4$ salt is reduced by Al according to the following reaction.

$$<2KBF_4> + \{3Al\} \Leftrightarrow <AlB_2> + 2KAlF_4 + Q$$

Depending upon the actual temperature at the interface, which shoots up due to the exothermic nature of the reaction, the aluminium boride intermetallic particles form. In case of Al-3B master alloys, the particles formed are $AlB_2$ and has been confirmed by X-ray diffraction studies. The EDX spectrum observed from the bulk of the sample are Al and B peaks. Analysis of the spectrum shows a B content of 2.75%, which is very close to that obtained by atomic absorption spectroscopy (2.71%). Figure 1b shows the EDX spectrum of Al-3B master alloy obtained from one of the $AlB_2$ particles. The quantitative analysis of the EDX spectrum has confirmed the particle to be $AlB_2$. Similarly, Al-3Ti and Al-5Ti master alloys were prepared and characterized by SEM/EDX analysis and $TiAl_3$ particles were found in these master alloys.

In case of Al-5Ti-1B master alloy, the following reaction takes place between Al and $K_2TiF_6$ and expected to release Ti in the solid form.

$$<3K_2TiF_6> + \{13Al\} \Leftrightarrow <3Al_3Ti> + <3KAlF_4> + <K_3AlF_6>$$

Figure 2a-c shows the SEM microphotograph and EDX spectrums of Al-5Ti-1B master alloy prepared at a reaction temperature of $800^0$C and with a reaction time of 60 min. The Figure 2a clearly revealed the presence of $Al_3Ti$ particles, among these large numbers of particles were blocky in nature. In addition, a number of fine particles were also observed. The EDX microanalysis of these fine particles revealed a high concentration of Ti (Figure 2b) suggesting that these fine particles could be $TiB_2$. The aluminium peak observed in the spectrum must have been originated from the interaction of the electron beam with the matrix, as the interaction volume is usually much bigger than the actual diameter of the electron beam. As the $TiB_2$ particles are very fine, the Al matrix below and surrounding them also contributes to the EDX spectrum. The EDX spectrum (at 20kv) of an $Al_3Ti$ particle is shown in Figure 2c and quantitative analysis has shown that the particle composition is very close to $Al_3Ti$. These results suggest that the alloy has mainly large $Al_3Ti$ particles at the centers of the α-Al grains and fine $TiB_2$ particles at the grain boundaries. The Al-5Ti-1B master alloy has been extensively investigated in the past by many workers and the findings in this part of the study are in close agreement with those of others. The Ti:B ratio (5:1) is >>0.5 and ensures the presence of $Al_3Ti$ and $TiB_2$ particles that was confirmed by XRD studies.

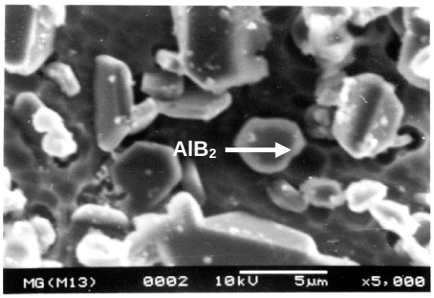


(a)

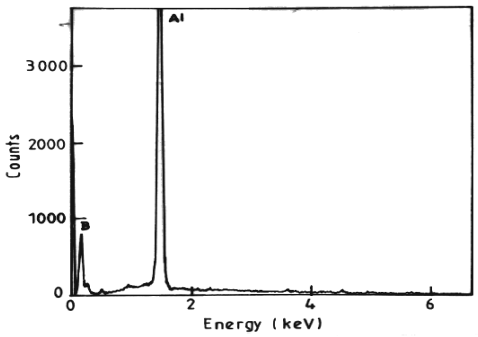


(b)

*Figure 1: Shows (a) SEM microphotographs of Al-3B master alloy revealing hexagonal $AlB_2$ particles and (b) EDX spectrum taken on $AlB_2$ particle.*

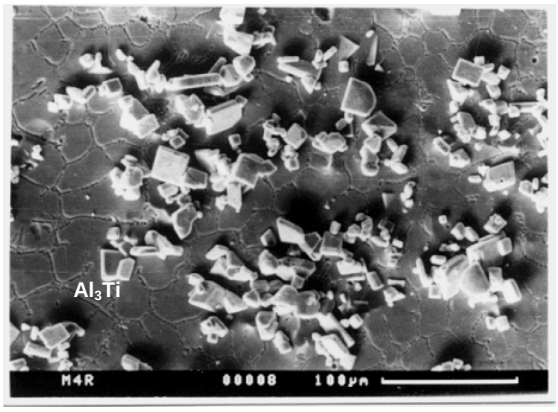


(a)

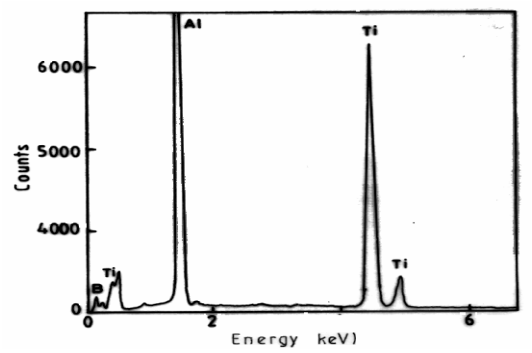


(b)

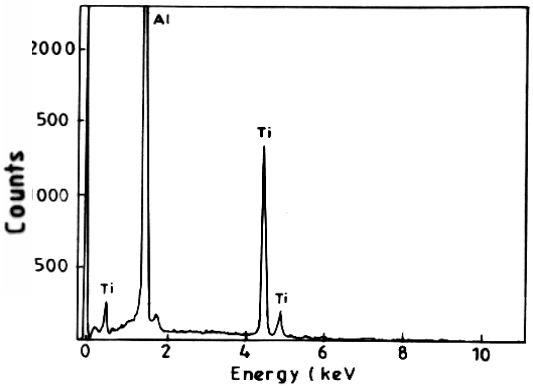


(c)

*Figure 2: Shows (a) SEM microphotographs of Al-5Ti-1B master alloy showing blocky $Al_3Ti$ particles and (b) EDX spectrum taken on bulk (c) EDX spectrum taken on $Al_3Ti$ particle.*

### 3.2 Grain Refinement Studies of Al-7Si alloy

Figure 3 shows the results of DAS analysis of Al-7Si alloy before and after the conventional addition levels (0.01%Ti and or B) of various Al-3Ti, Al-5Ti, Al-3B and Al-5Ti-1B master alloys. The figure clearly shows that in the absence of grain refiner the DAS value of Al-7Si alloy was 90µm (0 min.). With the addition of 0.35% (0.01%Ti) of Al-3Ti master alloy to the Al-7Si melt, the DAS decreases from 90µm to 66µm at shorter holding periods (2 min.). However, on longer holding periods (5-120min.), a continuous increase in DAS was observed from 70µm (5 min.) to 78µm (120 min.) indicating the dissolution/settling of the $Al_3Ti$ particles. Further stirring for 10 sec. after 120 min. casting resulted in some recovery of the $Al_3Ti$ particles in the melt, results in decreasing the size of the α-Al dendrites (64µm-120s min.). Similar results were obtained in Al-7Si alloy when grain refined with conventional addition level (0.01%Ti) of Al-5Ti, Al-5Ti-1B master alloys. However, addition of 0.40%(0.01%B) of Al-3B master alloy to Al-7Si alloy has resulted in decrease of DAS to 65, 65 and 63µm in case of 2, 120 and 120s min. of holding time respectively. Figure 3 also indicates that more dissolution/settling of $Al_3Ti$ particles observed in case of Ti-rich Al-3Ti, Al-5Ti and Al-5Ti-1B master alloys compared to B-rich Al-3B master alloy. This could be due to the density difference between $Al_3Ti$ (3.35g/cm$^3$) in Al-3Ti and Al-5Ti, $Al_3Ti$ (3.35g/cm$^3$) and $TiB_2$ (4.52 g/cm$^3$) in Al-5Ti-1B master alloys and $AlB_2$ (2.55g/cm$^3$) particles in Al-3B master alloy respectively.

Figure 4a-b shows the macrophotographs of Al-7Si alloy before and after the addition of optimum addition levels of 0.60% of Al-3B (0.016%B) and or 0.48% of Al-5Ti-1B (0.024%Ti) master alloys. Macrophotographs reveals that in the absence of grain refiner, Al-7Si alloy has shown coarse columnar structure (0min.). However, addition of Al-3B (0.60%) and Al-5Ti-1B (0.48%) master alloys to Al-7Si alloy resulted in complete conversion of coarse columnar structure to fine equiaxed structure at all holding times (2-120s min.). This could be due to the presence of $AlB_2$ and $Al_3Ti/TiB_2$ particles present in the master alloys (Al-3B and Al-5Ti-1B), and overcome the fading. This could be due to the more nucleating particles available for nucleation and resulted in less fading (Figure 5). In addition, higher addition level also leads to further decrease in size of α-Al dendrites compared to the conventional addition level (Figure 3). Further, macrophotographs also reveals that fine grain structure (Figure 4a) compared to (Figure 4b), suggesting Al-3B master alloy is more efficient than Al-5Ti-1B master alloy as explained above.

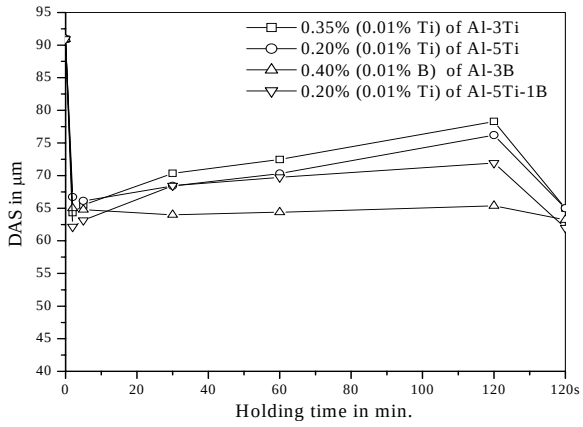


*Figure 3: Shows DAS analysis of Al-7Si alloy and grain refined with conventional addition levels of various master alloys.*

### 3.3 Microstructural Characterization

SEM/EDX analysis was carried out on Al-7Si alloy both in the absence and presence of grain refiner (Al-3B) to observe the microstructural changes and to identify the particles present in the alloy. Figure 6a and b shows SEM microphotographs of Al-7Si alloy without the grain refiner (0 min.) and with 0.60% of Al-3B master alloys. In the absence of grain refiner (Figure 6a) Al-7Si alloy shows elongated coarse columnar α-Al dendrites along with unmodified large eutectic Si needles/platelets at the grain boundaries. However, addition of 0.60% of Al-3B master alloys to Al-7Si alloy, resulted in the conversion of coarse columnar α-Al dendrites to fine equiaxed α-Al dendrites, while the eutectic Si remains more or less unaffected as expected and clearly observed in Figure 6b. Such structural conversion is due to the presence of $AlB_2$ particles present in the Al-3B master alloy. Figure 6c confirms the presence of these ($AlB_2$) particles at the centre of the α-Al matrix, which are responsible for heterogeneous nucleation during solidification.

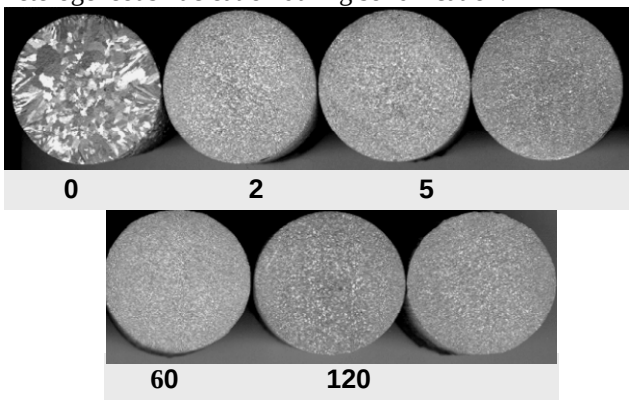


(a)

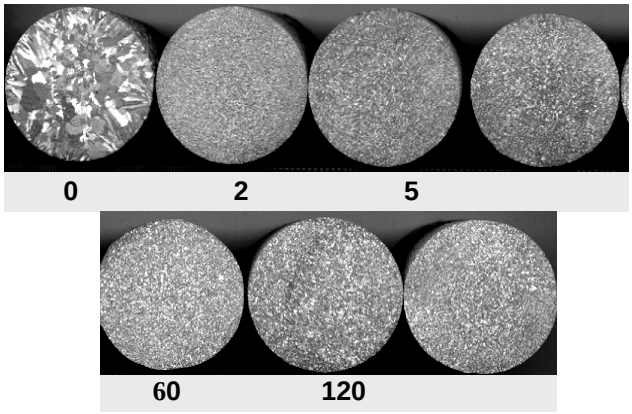


(b)

*Figure 4: Shows macrophotographs of Al-7Si alloy with (a) 0.60% of Al-3B and (b) 0.48% of Al-5Ti-1B master alloys.*

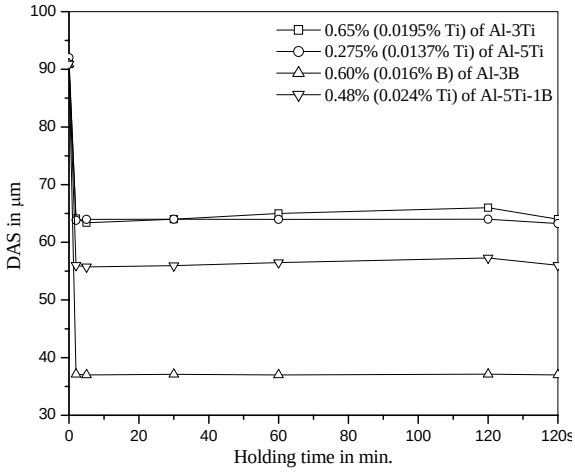


*Figure 5: Shows DAS analysis of Al-7Si alloy and grain refined with optimum addition levels of different master alloys.*

Figure 7a shows the SEM microphotograph of Al-7Si alloy grain refined with conventional addition level 0.2wt% (0.01%Ti) of Al-5Ti-1B master alloy. The figure clearly shows that the presence of complex aluminide particles containing Si, Ti and Fe at the grain boundaries of Al grains (Figure 7b). In addition, some of the Si particles observed in SEM were found to contain Ti and Fe as shown in Figure 7c.

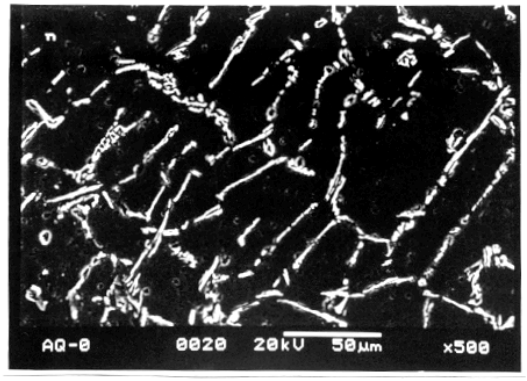


(a)

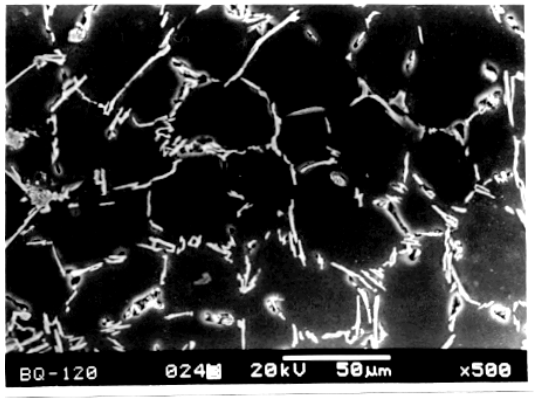


(b)

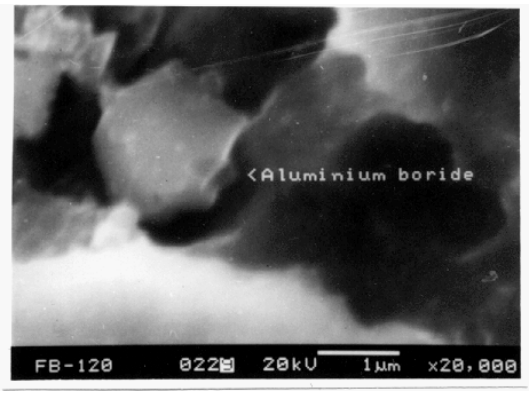


(c)

*Figure 6: a-c Shows SEM microphotographs of Al-7Si alloy (a) without grain refiner (b) with 0.60% of Al-3B (c) with 0.60% of Al-3B master alloy showing the presence of $AlB_2$ particles.*

These results suggest that Si and Fe dissolved in the melt react with the $TiAl_3$ particles and similarly some of the Si particles react with the Ti picked up by the melt owing to the dissolution of $TiAl_3$ particles. Further, the Ti $(Al,Si_3)$ phase existing in this system with Si soluble in $TiAl_3$ up to a composition of $Ti(Al_{0.8}Si_{0.2})_3$, also impacts negatively on the performance of grain refiner by altering the favorable lattice parameter of $TiAl_3$ [10]. However, in case of Al-7Si alloy grain refined with 0.48% (0.024%Ti) of Al-5Ti-1B master alloy, apart from complex aluminide particles, a few unreacted titanium aluminides were also observed. The improved grain refining response of Al-7Si alloy at higher addition level of the grain refiner could be due to the availability of some unreacted aluminide and boride particles that retain their potency for heterogeneous nucleation. A change in the surface chemistry of these particles by the reaction with poisoning elements such as Si can change $\gamma_{lp}$ (liquid particle interfacial energy) and or $\gamma_{sp}$ (solid particle interfacial energy) adversely, thus making them less potent nucleating sites which could be the cause for poor grain refining efficiency of the otherwise efficient grain refiner (Al-5Ti-1B) in the presence of Si.

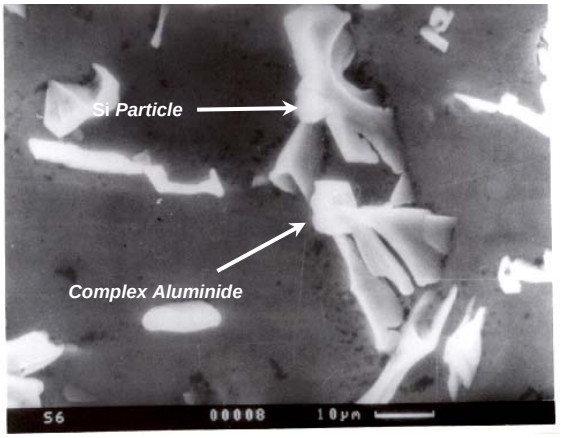


(a)

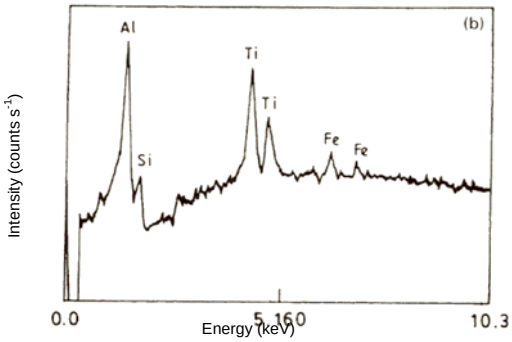


(b)

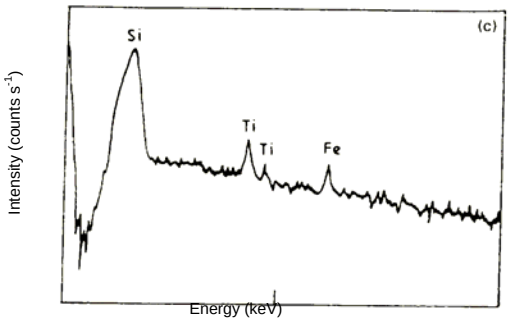


(c)

*Figure 7: a) shows SEM microphotograph of Al-7Si alloy grain refined with 0.2% of Al-5Ti-1B master alloy. b) EDX spectrum of titanium aluminide particle containing Si and Fe c) EDX spectrum of Si particle containing Ti and Fe [7].*

## 4. CONCLUSIONS

1. Fading of Al-7Si alloy is due to the settling of nucleating particles present in the master alloys.
2. Poisoning is essentially due to the formation of complex aluminides and silicides due to the interaction of Si with grain refining constituents present in the Ti-rich master alloys.
3. Vigorous agitation of the melt after prolonged holding (120 min.) can partly reduce the fading in Al-7Si alloy.
4. Higher addition levels of Ti-rich master alloys or B-rich Al-3B master alloys can overcome the poisoning effect and fading.
5. Al-7Si alloy shows better grain refining response towards B-rich master alloys when compared to Ti-rich master alloys.

## ACKNOWLEDGEMENTS

The first author is grateful to the Defence Research and Development Organization, Ministry of Defence, Government of India, New Delhi for providing the financial support towards carrying out the present work.

## REFERENCES


1. Bian Xiufang, Lin Xinhua and Liu Xiangfa, Jr. of Mat. Sci., vol. 33, 1998, pp 99-102.
2. B. S. Murty, S. A. Kori and M. Chakraborty, Int. Mater. Rev., vol-47, 2002, pp 3-29.
3. G. K. Sigworth and M .M. Guzowaski, AFS Trans. vol. 93, 1985, pp 907-912.
4. A. Cibula, J. Inst. Met. vol. 76, 1949-1950, pp 321-360.
5. M. E. J. Birch, and A. J. J. Cowell, Proc. of 4$^{th}$ Int. Conf. On Al-Li alloys, Paris, 1987, C3, pp 103-108.
6. J. A. Spittle and S. Sadli, Cast Met., vol. 7, 1995, pp 247-253.
7. S. A. Kori, B. S. Murty and M. Chakraborty, Mater. Sci. Technol., vol. 15, 1999, pp 986-992.
8. J. A. Spittle, J. M. Keeble, A. L. Meshhedani, TMS Light Metals, 1991, pp 795-800.
9. G. S. Vinod Kumar, B. S. Murty and M. Chakraborty, IFJ, vol. 49, 2003, pp 23-25.
10. P. Cooper, A. Hardman and Ed Burhop, TMS Light Metals, 2003 (1-6).
11. C. D. Mayes, D. G. McCartney, J. Tatlock, Mat. Sci. Tech., vol. 9, 1993, pp 97-103.
12. D. Boot, P. S. Cooper, D.H. St. John and A. K. Dahle, TMS Light Metals, 2002, pp 909.
13. A. L. Greer, T. E. Quested and J. E. Spalding, TMS Light Metals, 2002, pp 687.
14. T. E. Quested, A. L. Greer and P. S. Cooper, ICAA-8, 2002.
15. P. S. Mohanty, J. E. Gruzleski, Acta Mater, vol. 44, 1996, pp 3749-3760.